

STUDY OF ELECTRON DENSITY IN CAPILLARY DISCHARGE PLASMA FOR LASER PLASMA ACCELERATOR*

A. Whitehead^{1,2†}, S. Maity¹, M. Miceski^{1,2}, P. V. Sasorov¹, P. Zimmermann¹, S. Niekrasz¹,
J. T. Green¹, A. Jančárek^{1,2}, A. Molodozhentsev¹

¹ELI Beamlines Facility, The Extreme Light Infrastructure ERIC, Dolní Břežany, Czech Republic

²Czech Technical University in Prague, FNSPE, Prague, Czech Republic

Abstract

Gas-filled capillary discharge has emerged as a promising source in plasma-based accelerators. Pre-formed plasma channels enhance stability in Laser-Wakefield Accelerators by overcoming diffraction effects and maintaining laser focus over longer distances, thereby increasing energy transfer efficiency. Also, due to their limited gas consumption, they are well-suited for high repetition rate applications. Using Stark broadening, we measured profiles under varying conditions, achieving densities of $(2-3) \times 10^{18} \text{ cm}^{-3}$. Moreover, we present three-dimensional (3D) Particle-In-Cell (PIC) simulations incorporating experimentally measured plasma density profiles. The simulation results reveal electron injection and acceleration, with electrons attaining a mean energy of 0.5 GeV using a laser pulse of 2.0 J energy. This type of plasma source is a crucial technology for the 100 Hz plasma accelerator-based Free Electron Laser (FEL) being developed at ELI-ERIC and for the EuPRAXIA project.

INTRODUCTION

Plasma-based accelerators (PBAs) have demonstrated the ability to accelerate electrons either by using ultra-intense laser pulses, as in laser wakefield acceleration (LWFA) [1], or by employing charged particle beams to drive plasma waves, as in plasma wakefield acceleration (PWFA) [2].

Recent developments in PBAs community have achieved long term shot-to-shot stability [3] and high quality electron beam [4], reaching parameters suitable for Free Electron Laser (FEL) applications [5] [6]. The generation of high-repetition-rate electron beams, required for many applications, using emerging 100 TW-class laser systems operating at 100 Hz [7] remains one of the most interesting aspects of current research. However, transitioning to high-repetition operation imposes dual challenges: laser systems must reliably deliver ultrashort pulses, while target systems require plasma sources capable of sustaining high repetition rate operation.

In this work, we propose the use of a gas-filled capillary in which the plasma is generated by applying a high voltage electrical pulsed discharge. In a previously published paper, a three-dimensional magnetohydrodynamics simulations of a hydrogen gas filling process and discharge plasma forma-

tion was performed in [8]. This approach ionises the gas and creates a plasma channel that acts as a waveguide for the laser pulse. The preformed plasma channel allows the laser to propagate over longer distances within the plasma, compared to channels ionised solely by the laser pulse, effectively overcoming diffraction limitations. Enabling the possibility to use laser systems with lower peak power [9] thus making the high repetition rates accessible. Furthermore, these channels enhance the efficiency of energy transfer from the laser pulse to the plasma wave, resulting in lower transmission and coupling losses [10]. When the capillary is filled with hydrogen, the plasma can be fully ionised, which helps to minimise both spectral and temporal distortions of the guided laser pulse [11, 12].

Longitudinal plasma density profiles were obtained from time-resolved emission spectroscopy, utilising Stark broadening analysis of the hydrogen Balmer- α ($H\alpha$) line at 656.3 nm. Complementary 3D particle-in-cell (PIC) simulations, incorporating experimentally measured plasma density profiles, confirm the gas filled capillary discharge's ability to produce GeV-class electron beams.

DENSITY MEASUREMENT METHOD

Experimental Setup

The plasma source characterised in this study is a 15 mm long sapphire capillary with a square cross-section of $300 \times 300 \mu\text{m}$, filled with hydrogen. The hydrogen is supplied continuously from an electrolytic generator and introduced into the capillary via two inlets, with the flow regulated by two independent mass flow controllers. The experimental setup is shown in Fig. 1. Plasma is generated by applying a high-voltage electrical discharge, with a duration of approximately 300 ns (full width at half maximum (FWHM)), across two electrodes placed at each end of the capillary. This discharge provides a current of about 300 A at 25 kV. The light emitted from the plasma is collected and then focused into a spectrometer (*Andor Kymera 328i*). The collected light is dispersed by a diffraction grating with 1200 lines/mm and recorded by an intensified scientific Complementary Metal-Oxide-Semiconductor (sCMOS) camera (*Andor iStar*). An internal delay can be introduced to measure the temporal evolution of the plasma.

For the experiments presented in this paper, we selected the hydrogen $H\alpha$ line at 656.3 nm because it has a higher transition probability compared to the hydrogen Balmer- β line at 486.1 nm, thereby enhancing the signal-to-noise ratio.

* This work was supported by the European Union's Horizon Europe research and innovation programme under grant agreement no. 101073480 and the UKRI guarantee funds, and by the Ministry of Education, Youth and Sports of the Czech Republic through the e-INFRA CZ (ID:90254).

† alex.whitehead@eli-beams.eu

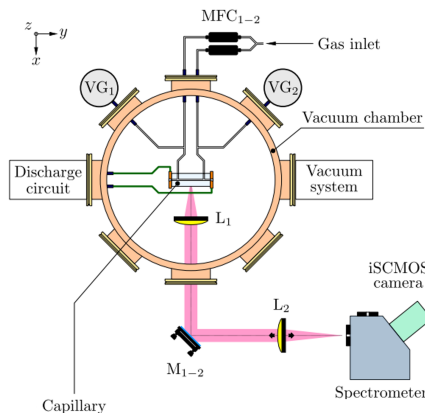


Figure 1: Schematic diagram of the experimental setup. Labels: MFC - mass flow controller, VG - vacuum gauge, L - lens, M - mirror.

Stark Broadening Method

The application of a high-voltage electrical discharge to the electrodes induces rapid electron temperature elevation, driving gas ionisation through collisional processes [12]. This results in a plasma that is either fully or partially ionised, depending on discharge parameters.

The Stark broadening method exploits spectral line broadening caused primarily by microscopic electric field fluctuations within the plasma [13]. Plasma electron density n_e is determined from the spectral line width using the relation [14]:

$$n_e [\text{cm}^{-3}] = 8.02 \times 10^{12} \left(\frac{\Delta \lambda_{FWHM}}{\alpha_{H\alpha}} \right)^{3/2}, \quad (1)$$

where $\Delta \lambda_{FWHM}$ represents the FWHM of the Stark-broadened spectral line in angstroms, and the constant $\alpha_{H\alpha} = 0.0214$ denotes the fractional intensity width of the $H\alpha$ line, derived from electron temperature and density dependencies [15]. As shown in Eq. 1, broader spectral line widths measured by the camera correspond directly to higher electron densities.

EXPERIMENTAL RESULTS

Using the experimental setup described in the previous section, we measured longitudinal electron density profiles by systematically varying both the camera's internal delay timing and the gas flow through the inlets.

Figure 2 shows the maximum electron densities measured at flow rates of 0.150 mg/s and 0.075 mg/s per inlet. The peak plasma densities reached $2.4 \times 10^{18} \text{ cm}^{-3}$ and $1.3 \times 10^{18} \text{ cm}^{-3}$, respectively. These values fall within the typical range for laser waveguiding in plasma channels (10^{17} - 10^{18} cm^{-3}), confirming that the discharge plasma satisfies this condition. However, optimal electron acceleration in LWFA requires operation within the 10^{18} cm^{-3} range, where the wakefield's accelerating gradient scales as $E \propto \sqrt{n_e}$. This density regime is localised between the gas inlets, limiting

the effective accelerating region to approximately 60 % of the capillary length.

Figure 2(a) exhibits a higher density compared to Fig. 2(b), consistent with the measured pressures of 170 mbar and 110 mbar, respectively. However, the higher flow regime showed increased instabilities, likely due to incomplete ionisation within the channel. As the discharge current rises, it may remain insufficient to fully ionise the bulk gas before thermal equilibrium is achieved [10].

The impact of these density fluctuations on LWFA performance is investigated via 3D PIC simulations in the following section.

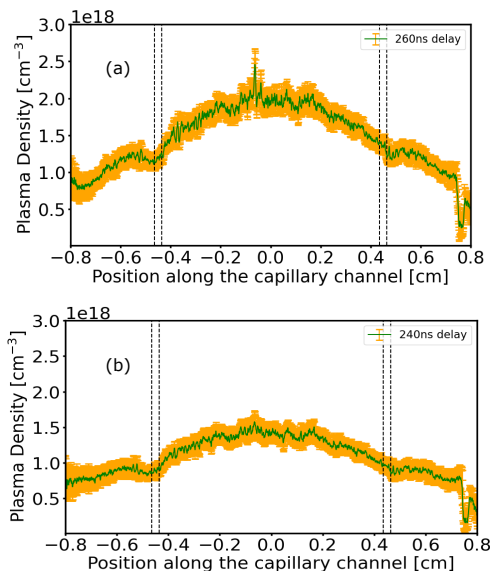


Figure 2: Longitudinal plasma density profiles averaged over 50 images for gas inlet flows of (a) 0.150 mg/s and (b) 0.075 mg/s. Discharge parameters: 25 kV voltage, ~ 300 A current. Dashed black regions indicate gas inlet positions. Top-right values denote camera acquisition delays (10 ns resolution) relative to discharge triggering.

PIC SIMULATIONS

Particle-in-cell (PIC) simulations were performed using *SMILEI* code [16] in a quasi-3D (azimuthal symmetry) geometry. A moving window with speed c was used in the simulation, with a transverse radius of 100λ (grid resolution $\lambda/10$) and a length of 80λ (grid resolution $\lambda/50$), and a time step of $\lambda/51c$. The driver laser is considered a Gaussian pulse, linearly polarized along the y direction and propagating in the x direction. The laser parameters used in the simulation are the following: 820 nm wavelength, 2 J energy, 30 fs pulse duration (FWHM), and $20 \mu\text{m}$ beam waist. The laser was initially focused at a position $x = 8.0$ mm (Fig. 3(a)). The experimentally measured plasma density profile, shown in Fig. 2, was used as input for the simulation. In the transverse direction, a parabolic density profile of the form $n_e(r) = n_e(0)[1 + 0.33(r^2/R_0^2)]$, where $R_0 = 300 \mu\text{m}$ is the capillary radius, was assumed [12].

The simulation results are shown in Figs. 3 and 4. In Fig. 3(a), the on-axis plasma density profile extracted from the PIC simulation, along with the evolution of the normalized vector potential a_0 as a function of laser propagation distance, has been shown. Since the laser power exceeds the critical power for relativistic self-focusing by approximately a factor of 5.0 in the plasma plateau region between $x \approx 6.0$ mm and 11 mm, the laser pulse undergoes self-focusing. As a result, a_0 increases beyond its vacuum focus value (around 2.3) and remains nearly constant throughout this density plateau. Electrons are injected and trapped within the first bubble behind the laser pulse, as illustrated in Fig. 3(b). The net injected charge in the first bubble is approximately 60 pC.

The electron beam accelerated in the first bubble behind the driver laser pulse is characterized after exiting the plasma at $x = 17.5$ mm, as shown in Fig. 4. The simulation results demonstrate that a 15 mm-long capillary discharge, driven by a 2.0 J laser pulse, can produce electron beams with a charge of 60 pC, a mean energy of 525 MeV with an RMS energy spread of approximately 25%. The resultant beam has an RMS divergence of approximately 1.3 mrad horizontally and 1.4 mrad vertically, with corresponding RMS normalised beam emittances of 1.8 mm-mrad and 2.2 mm-mrad, respectively.

Our PIC simulations (not presented here) suggest that increasing the laser energy significantly boosts the beam charge. For example, at a laser energy of 3.0 J, the net accelerated charge can attain levels as high as 600 pC, with mean energies ranging between 300 and 500 MeV. However, in this case, the quality of the beam, particularly the RMS energy spread, divergence, and emittance, degrades considerably due to the beam overloading effect. These high-charge accelerated electron beams would have promising applications in a hybrid staged laser and plasma accelerator setup [17], where they could serve as drivers for the plasma wakefield acceleration stage. Our simulation observations also indicate that the position of the laser focus plays a crucial role in achieving optimal acceleration. We found that when the laser is focused at the beginning of the capillary (for example, at $x = 2.0$ mm), a substantial number of electrons (with a net charge ranging from 400-500 pC, even at 2.0 J of laser energy) are injected into the first wake structure. However, as the laser propagates and the plasma density increases, the wavelength of the wake structure decreases. Consequently, electrons injected in the first wake structure, slip into the second bubble, where they experience a decelerating and defocusing phase of the wake electric field. This leads to a minimal final energy gain for the beam and significantly deteriorates its quality.

CONCLUSION AND PERSPECTIVES

We have presented the characterisation of the longitudinal plasma density profile for a 15 mm long sapphire capillary, achieving a peak density of $2.4 \times 10^{18} \text{ cm}^{-3}$ under the discharge conditions of 25 kV and 0.150 mg/s per gas inlet. The

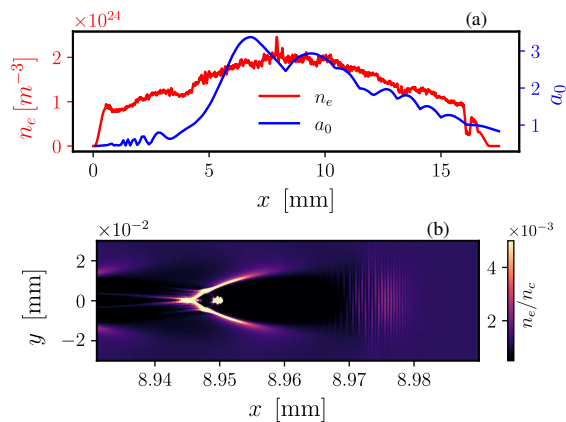


Figure 3: (a) On-axis plasma density n_e (red) and peak normalized vector potential a_0 (blue) as a function of laser propagation distance. (b) Plasma electron density in the x-y plane at a particular simulation time shows electron injection in the first wake structure behind the laser pulse.

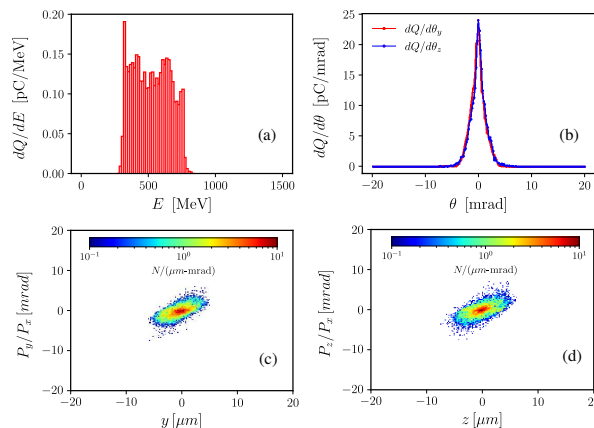


Figure 4: Electron beam parameters at the end of plasma, i.e., $x = 17.5$ mm: (a) Energy spectrum, (b) divergence in (red) horizontal and (blue) vertical directions, and emittance in (c) the horizontal and (d) in the vertical plane.

results reveal a stable high-density region over 10^{18} cm^{-3} covering 60% of the capillary length. This finding motivates further studies with extended capillaries to fully exploit the accelerating potential over longer interaction lengths.

3D PIC simulations utilizing the experimentally measured density profile demonstrated an effective acceleration of electron beams along the plasma channel, achieving a mean energy of 0.5 GeV. Although the transverse properties of the accelerated electron beams are reasonably good, the energy spread remains high and is therefore incompatible with the requirements for FEL. By optimizing capillary geometries and adjusting gas parameters, such as pressure gradients and gas mixtures, it would be possible to refine the density profiles and produce electron beams that meet FEL specifications.

REFERENCES

- [1] T. Tajima and J. M. Dawson, “Laser electron accelerator”, *Phys. Rev. Lett.*, vol. 43, pp. 267–270, 1979. doi:10.1103/PhysRevLett.43.267
- [2] P. Chen, J. M. Dawson, R. W. Huff, and T. Katsouleas, “Acceleration of electrons by the interaction of a bunched electron beam with a plasma”, *Phys. Rev. Lett.*, vol. 54, pp. 693–696, 1985. doi:10.1103/PhysRevLett.54.693
- [3] S. Bohlen, J. C. Wood, T. Brümmer, F. Grüner, C. A. Lindström, M. Meisel, T. Staufer, R. D’Arcy, K. Pöder, and J. Osterhoff, “Stability of ionization-injection-based laser-plasma accelerators”, *Phys. Rev. Accel. Beams*, vol. 25, pp. 031301, 2022. doi:10.1103/PhysRevAccelBeams.25.031301
- [4] W. T. Wang, W. T. Li, J. S. Liu, Z. J. Zhang, R. Qi, C. H. Yu, J. Q. Liu, M. Fang, Z. Y. Qin, C. Wang, Y. Xu, F. X. Wu, Y. X. Leng, R. X. Li, and Z. Z. Xu, “High-Brightness High-Energy Electron Beams from a Laser Wakefield Accelerator via Energy Chirp Control”, *Phys. Rev. Lett.*, vol. 117, pp. 124801, 2016. doi:10.1103/PhysRevLett.117.124801
- [5] W. Wang, K. Feng, L. Ke, C. Yu, Y. Xu, R. Qi, Y. Chen, Z. Qin, Z. Zhang, M. Fang, J. Liu, K. Jiang, H. Wang, C. Wang, X. Yang, F. Wu, Y. Leng, J. Liu, R. Li, and Z. Xu, “Free-electron lasing at 27 nanometres based on a laser wakefield accelerator”, *Nature*, vol. 595, pp. 516–520, 2021. doi:10.1038/s41586-021-03678-x
- [6] R. Pompili, D. Alesini, M. P. Anania, S. Arjmand, M. Behtouei, M. Bellaveglia, ... and M. Ferrario, “Free-electron lasing with compact beam-driven plasma wakefield accelerator”, *Nature*, vol. 605, pp. 659–662, 2022. doi:10.1038/s41586-022-04589-1
- [7] J. T. Green, R. Antipenkov, P. Bakule, and B. Rus, “L2-DUHA 100 TW high repetition rate laser system at ELI-Beamlines. Key design considerations”, *Rev. Laser Eng.*, vol. 49, pp. 106–109, 2021. doi:10.2184/laj.49.2_106
- [8] G. A. Bagdasarov, K. O. Kruchinin, A. Y. Molodozhentsev, P. V. Sasorov, S. V. Bulanov, and V. A. Gasilov, “Discharge plasma formation in square capillary with gas supply channels”, *Phys. Rev. Res.*, vol. 4, pp. 013063, 2022. doi:10.1103/PhysRevResearch.4.013063
- [9] E. Cormier-Michel, V. H. Ranjbar, D. L. Bruhwiler, J. R. Cary, M. Chen, C. G. R. Geddes, G. R. Plateau, N. H. Matlis, and W. P. Leemans, “Design principles for high quality electron beams via colliding pulses in laser plasma accelerators”, *Phys. Rev. ST Accel. Beams*, vol. 17, pp. 091301, 2014. doi:10.1103/PhysRevSTAB.17.091301
- [10] K. O. Kruchinin, A. Mondal, P. V. Sasorov, P. Zimmermann, S. Niekrasz, and A. Yu. Molodozhentsev, “Experimental characterization of discharge plasma dynamics in a square capillary for prospective applications in laser wakefield acceleration”, *Phys. Plasmas*, vol. 32, pp. 043511, 2025. doi:10.1063/5.0260100
- [11] K. Nakamura, B. Nagler, C. Tóth, C. G. R. Geddes, C. B. Schroeder, E. Esarey, W. P. Leemans, A. J. Gonsalves, and S. M. Hooker, “GeV electron beams from a centimeter-scale channel guided laser wakefield accelerator”, *Phys. Plasmas*, vol. 14, 2007. doi:10.1063/1.2718524
- [12] N. A. Bobrova, A. A. Esaulov, J.-I. Sakai, P. V. Sasorov, D. J. Spence, A. Butler, S. M. Hooker, and S. V. Bulanov, “Simulations of a hydrogen-filled capillary discharge waveguide”, *Phys. Rev. E*, vol. 65, pp. 016407, 2001. doi:10.1103/PhysRevE.65.016407
- [13] I. I. Sobelman, “Atomic Spectra and Radiative Transitions”, *Atomic Spectra and Radiative Transitions*, 1992. doi:10.1007/978-3-642-76907-8
- [14] D. G. Jang, M. S. Kim, I. H. Nam, H. S. Uhm, and H. Suk, “Density evolution measurement of hydrogen plasma in capillary discharge by spectroscopy and interferometry methods”, *Appl. Phys. Lett.*, vol. 99, 2011. doi:10.1063/1.3643134
- [15] H. R. Griem, “Spectral line broadening by plasmas”, *Spectral Line Broadening by Plasmas*, 1974. doi:10.1017/cbo9780511524578.005
- [16] J. Derouillat, A. Beck, F. Pérez, T. Vinci, M. Chiaramello, A. Grassi, ... and M. Grech, “SMILEI: A collaborative, open-source, multi-purpose particle-in-cell code for plasma simulation”, *Comput. Phys. Commun.*, vol. 222, pp. 351–373, 2018. doi:10.1016/j.cpc.2017.09.024
- [17] F. M. Foerster, A. Döpp, F. Haberstroh, K. v. Grafenstein, D. Campbell, Y. Y. Chang, ... and S. Karsch, “Stable and High-Quality Electron Beams from Staged Laser and Plasma Wakefield Accelerators”, *Phys. Rev. X*, vol. 12, pp. 041016, 2022. doi:10.1103/PhysRevX.12.041016